Original Article

Towards grain-scale modelling of the release of radioactive fission gas from oxide fuel. Part I: SCIANTIX

G. Zullo [a], D. Pizzocri [a], A. Magni [a], P. Van Uffelen [b], A. Schubert [b], L. Luzzi [a, *]

[a] Politecnico di Milano, Department of Energy, Nuclear Engineering Division, Via La Masa 34, 20156, Milano, Italy
[b] European Commission, Joint Research Centre (JRC), Karlsruhe, Germany

ARTICLE INFO

ABSTRACT

When assessing the radiological consequences of postulated accident scenarios, it is of primary interest to determine the amount of radioactive fission gas accumulated in the fuel rod free volume. The state-of-the-art semi-empirical approach (ANS 5.4−2010) is reviewed and compared with a mechanistic approach to evaluate the release of radioactive fission gases. At the intra-granular level, the diffusion-decay equation is handled by a spectral diffusion algorithm. At the inter-granular level, a mechanistic description of the grain boundary is considered: bubble growth and coalescence are treated as inter-related phenomena, resulting in the grain-boundary venting as the onset for the release from the fuel pellets. The outcome is a kinetic description of the release of radioactive fission gases, of interest when assessing normal and off-normal conditions. We implement the model in SCIANTIX and reproduce the release of short-lived fission gases, during the CONTACT 1 experiments. The results show a satisfactory agreement with the measurement and with the state-of-the-art methodology, demonstrating the model soundness. A second work will follow, providing integral fuel rod analysis by coupling the code SCIANTIX with the thermo-mechanical code TRANSURANUS.

1. Introduction

Evaluating the radiological consequences of the release of short-lived fission gases from nuclear power plants is an important task, especially after the Three Mile Island accident [1], Chernobyl and the Fukushima Daiichi accident [2,3]. European and international research programs (through FP7 and H2020 frameworks, as well as OECD/NEA/CSNI organizations) aim to improve the determination of such radiological consequences and to identify proper mitigation strategies by integration with probabilistic safety assessments [4]. At present, the estimation of the amount of radioactive fission gases released from the nuclear fuel is obtained by considering very conservative deterministic assumptions. Quantifying the effective gains introduced by additional safety measures is not a straightforward task when such conservative assumptions are involved.

This work is part of the Reduction of Radiological Consequences of design basis and extension Accidents (R2CA) European H2020 project [5]. In particular, Loss of Coolant Accidents (LOCA) and Steam Generator Tube Rupture (SGTR) accidents, in Pressurized Water Reactor (PWR) and Boiling Water Reactor (BWR) conditions are addressed in R2CA framework. The main objectives of the R2CA project can be summarized as the comparison of state-of-the-art methodologies with existing experimental data and tools to assess the degree of conservativism and derive more realistic safety margins for design basis accidents. Research programs put great efforts towards the development of improved mechanistic models that can be employed in fuel performance codes (FPCs) such as TRANSURANUS [6,7] to enhance the description of nuclear fuel rod behaviour during both normal and off-normal conditions.

In general, a crucial task is the determination of the source term, i.e., the radioactivity that can be released from the reactor containment to the environment and population [8,9]. For this purpose, the rate of radioactive fission gases released from the fuel has been investigated. The release rates of radioactive fission gases from fuel rods are determined from integral simulation codes (e.g., ASTEC [10], MELCOR [11]). The amount of released radioactive gases depends on the behaviour of the nuclear fuel during the reactor operation. Empirical or semi-empirical correlations can estimate the amount of released fission gases accumulated in the fuel rod free volume. These empirical correlations are typically tailored to reproduce normal reactor operations and do not model the time-

dependent behaviour of the released fission gases. Physics-based models aim to overcome some of these limitations.

In this work, the behaviour of radioactive fission gases (xenon and krypton isotopes) is addressed. We aim to predict the amount of fission gases of radiological concern that are released from the fuel pellets and accumulated in the fuel rod free volume. We exploit a mechanistic model to describe the behaviour of fission gases, including the fundamental role played by intra- [12] and inter-granular bubbles [13] filled with fission gases. Indeed, at the intra-granular level, the diffusion-decay equation is handled with a spectral solver, for which the bound on the numerical error provides a quality assurance on the computed concentration of several short-lived fission gases [14]. At the same time, we consider the accumulation of fission gases in grain-boundary bubbles, the resulting bubble growth and coalescence until a grain-boundary saturation threshold is attained. The release of fission gases from these bubbles results from the venting of interconnected grain-boundary bubbles. The main outcome is a kinetic description of the fractional release.

In principle, our model is able to reproduce the behaviour of short-lived fission gases in both stationary and transient power conditions, hence the evaluation of the radioactivity accumulated in the fuel rod free volume. Nevertheless, experimental data to validate our predictions are essential. To the best of the authors' knowledge, the CONTACT experiments are one of the few campaigns in open literature that are reproducible and that focus on the radioactive fission gases accumulated in the fuel rod free volume under normal operating conditions. Hence, they can be compared with the predictions of a model targeting only the fuel behaviour.

We first consider some short-lived isotopes of xenon and krypton, the same that are monitored in the CONTACT experiments. Our model and its predictions are also compared with the state-of-the-art methodology ANS 5.4–2010 [15], semi-empirical and calibrated on experimental data, able to predict the fractional release of short-lived (radioactive isotopes with half-life shorter than one year) fission gases, accumulated in the fuel rod free volume, in stationary conditions.

We implement our model in SCIANTIX, a 0D computer code designed to be coupled with existing FPCs as a fission gas behaviour module [16]. The coupling of SCIANTIX with TRANSURANUS and GERMINAL has been successfully performed [17] and future coupling with other FPCs (e.g., BISON [18,19]) are ongoing tasks. Moreover, a second work will follow the present one, providing additional integral fuel rod analysis thanks to the coupling of SCIANTIX with the code TRANSURANUS.

The present work is structured as follows. In Section 2, we describe the state-of-art-methodology ANS 5.4–2010, used to predict the fractional release of short-lived volatile fission gases of primary radiological concern. We point out the main assumptions and limitations of the methodology. Then, we depict the mechanistic treatment of radioactive volatile fission gases, based on the current descriptions of inter-granular bubble behaviour [13]. We provide a kinetic evaluation of the fractional release of radioactive volatile fission gases. In Section 3, we test our model and the ANS 5.4–2010 methodology against the CONTACT experiments, comparing the results with the available experimental data. Conclusions are drawn in Section 4.

2. Modelling of radioactive fission gas release

The release of fission gases from the fuel to the fuel rod free volume is currently modelled with a two-step process [20–22].

1. Fission gas atoms (both stable and radioactive isotopes) are uniformly generated in the fuel grains, due to nuclear fission

events, with determined isotopic yields. The dominant transport mechanism from the fuel matrix to the fuel rod free volume, is the atomic diffusion [13,22–24], in the first place from within the grains to the grain boundaries. In particular, the intra-granular diffusion of fission gas towards grain boundaries causes their accumulation in grain-boundary bubbles.

2. The inter-granular bubbles grow by absorption of both fission gas and vacancies and can coalesce together, resulting in larger and fewer bubbles [24]. Coherently with the state-of-the-art modelling [13,22,24] we assume that this process continues until the grain boundaries are sufficiently populated with large bubbles, and a network of interconnected bubbles is formed. This network constitutes a pathway through which fission gas is vented out the fuel pellet, as soon as the network gets in touch with an easy escape route, e.g., a fuel crack. We assume that this release happens instantly, i.e., the gas is brought from the grain boundaries to the fuel rod free volume, neglecting all the intermediate mechanisms occurring[1] [25]).

The aforementioned behaviour is supported by experimental observations of fractured surfaces of UO_2 showing that the grain boundaries are populated by large, lenticular bubbles [24]. A satisfactory modelling approach for the grain face bubble coalescence has been described in Refs. [13,24,26] and it is summarized in Sec. 2.2. Moreover, if we consider the grain-boundary bubble density N_{gb} (bub m^{-2}) and the bubble average (projected on the grain boundary) area A_{gb} (m^2), it is possible to define the projected-area coverage fraction of the grain boundary with grain boundary bubbles as $N_{gb}A_{gb}$. The latter quantity is defined as fractional coverage F_c (/). The critical, or saturation, value of F_c that determines the interconnection of the grain boundary bubbles is set to $F_c = 0.5$ [24,27].

2.1. State-of-the-art model: ANS 5.4–2010

Given the importance of evaluating the amount of short-lived fission gas isotopes accumulated in the fuel rod free volume, the American Nuclear Society (ANS) provided a semi-empirical methodology (to which we refer in the present work as the ANS 5.4–2010 methodology [15]) for evaluating the release-to-birth ratio of short-lived fission gases of radiological concern (Table 1). This methodology is applicable to Light Water Reactors (LWRs), working in nominal, stationary conditions. If coupled with isotopic yields, ANS 5.4–2010 provides the *gap activity*, which is the inventory of radioactive fission gas isotopes that accumulates in the fuel rod free volume and is available to be released from the fuel rod if the cladding is breached. The current ANS 5.4–2010 methodology applies only to short-lived (defined as the ones with half-life shorter than one year) fission gas isotopes, of primarily radiological interest, namely krypton, xenon and iodine isotopes (Table 1). Different methodologies are required to determine the release of long-lived fission gases, such as ^{85}Kr. We report the ANS 5.4–2010 basic modelling approach and parameters for evaluating the release-to-birth ratio of short-lived fission gases (see Table 2).

2.1.1. Intra-granular behaviour of radioactive fission gases
The ANS 5.4–2010 methodology starts from the simplified

---

[1] The mechanistic model that we present in the next section (Section 2.2) neglects the mechanisms related to the tunnel formation along grain edges, grain-face diffusion, departure from lenticular shape of grain-face bubbles, irradiation-induced re-solution of fission gas atoms from the grain faces to the grain interior, presence of single atoms at the grain boundaries (instantaneous trapping). These assumptions are in line with [13] and with the SCIANTIX validation [16].

Table 1
Decay rates, half-lives and precursor enhancement factors (α) for radioactive fission gases considered in the ANS 5.4–2010 methodology [15].

Nuclide	Decay rate (s^{-1})	Half-life	α (−)
^{85m}Kr	4.30×10^{-5}	4.48 h	1.31
^{87}Kr	1.52×10^{-4}	1.27 h	1.25
^{88}Kr	6.78×10^{-5}	2.84 h	1.03
^{89}Kr	3.35×10^{-3}	3.15 min	1.21
^{90}Kr	2.15×10^{-2}	32.3 s	1.11
^{131}I	9.98×10^{-7}	8.04 d	1.0
^{132}I	8.44×10^{-5}	2.28 h	137
^{133}I	9.26×10^{-6}	20.8 h	1.21
^{134}I	2.20×10^{-4}	52.6 min	4.4
^{133}Xe	1.53×10^{-6}	5.243 d	1.25
^{135m}Xe	7.55×10^{-4}	15.3 min	23.5
^{135}Xe	2.12×10^{-5}	9.10 h	1.85
^{137}Xe	3.03×10^{-3}	3.82 min	1.07
^{138}Xe	8.19×10^{-4}	14.1 min	1.00
^{139}Xe	1.75×10^{-2}	39.7 s	1.00

Table 2
List of the parameters used in the ANS 5.4–2010 methodology to estimate the release-to-birth ratio of short-lived fission gases [15].

Symbol	Definition/value	Units	Reference
λ	Decay rate	s^{-1}	[41]
α	Precursor enhancement factor	(−)	[15,23]
D	Single-atom diffusivity in UO$_2$	m^{2}s^{-1}	[15]
	$D_1 + D_2 + D_3$		
	$D_1 = 7.6e - 11 \exp(-35\,000/T)$		
	$D_2 = 1.41e - 25\sqrt{\dot{F}}\exp(-13\,800/T)$		
	$D_1 = 2e - 40\dot{F}$		
	$\dot{F}$ (fiss m^{-3} s^{-1}), fission rate density		
	T (K), local fuel temperature		
S/V	Surface-to-volume ratio of the fuel sample	m^{-1}	[15,34,37]
T_{IC}	Interconnection temperature	m^{-1}	[15,36]

intra-granular diffusive problem of radioactive fission gas, according to the Booth formulation [28]. Hence, fission gas is uniformly produced at a rate $B = yF$ (at m^{-3} s^{-1}), y (at fiss^{-1}) being the isotopic yield and F (fiss m^{-3} s^{-1}) the fission rate density, in a spherical domain of equivalent radius a (m). The diffusion towards the spherical boundary is regulated by the following equation:

$$\frac{\partial C(r,t)}{\partial t} = \frac{D_{\text{eff}}}{r^2} \frac{\partial}{\partial r}\left(r^2 \frac{\partial C(r,t)}{\partial r}\right) - \lambda C(r,t) + B \tag{1}$$

where $C(r, t)$ (at m^{-3}) is the intra-granular concentration of the radioactive fission gas under investigation, whose decay rate is λ (s^{-1}). D_{eff} (m^2 s^{-1}) is the effective intra-granular diffusivity of the atoms in the fuel matrix. According to ANS 5.4–2010 treatment, $D_{\text{eff}} = \alpha D$, where D is the single-atom diffusivity in uranium dioxide and α is the precursor enhancement factor, explained later in the text. The accurate derivation of $C(r, t)$ and the release-to-birth ratio R/B from Eq. (1) is described in Beck's work [29].

The ANS 5.4–2010 methodology assumes the secular equilibrium of the reactor (i.e., when the reactor operates at constant power for at least three half-times of the considered isotope). Under this assumption, the release-to-birth ratio R/B is given by the following expression:

$$\frac{R}{B} = \frac{3}{\sqrt{\mu}}\left(\coth\sqrt{\mu} - \frac{1}{\sqrt{\mu}}\right) \tag{2}$$

which depends on the dimensionless group $\mu = \lambda a^2/D_{\text{eff}}$. The release rate R (at m^{-3} s^{-1}) is obtained from the concentration gradient at the boundary of the spherical ideal grain ($r = a$), i.e., $R \equiv$

$- D_{\text{eff}}\frac{3}{a}\frac{\partial C(r,t)}{\partial r}\Big|_{r=a}$. If the equivalent radius a is replaced with the surface-to-volume ratio $S/V = 3/a$ we get for μ:

$$\mu = \frac{9\lambda}{(S/V)^2 \alpha D} \tag{3}$$

Eq. (2) can be further simplified if R/B is small enough, i.e., $R/B < 2\%$, that is whenever $\mu > 22\,000$:

$$\frac{R}{B} \approx \frac{3}{\sqrt{\mu}} = \frac{S}{V}\sqrt{\frac{\alpha D}{\lambda}} \tag{4}$$

this approximation is valid with a small excess relative error, less than 10^{-2}.

The intra-granular diffusive process of each radioactive fission gas depends both on the single-atom diffusivity D (m^2 s^{-1}) in the uranium dioxide matrix and on its radioactive precursor, by means of the precursor enhancement factor α. Following the work of Turnbull, Friskney and co-workers on the release of stable and unstable fission gases in a wide range of temperatures from single and polycrystalline UO$_2$ during irradiation [30–32], a semi-analytic formulation of D was given as:

$$D = 7.6e - 10^{-10}e^{-35\,000/T} + 5.64e - 10^{-25}\sqrt{\dot{F}}e^{-13\,800/T} + 2e$$
$$- 10^{-40}\dot{F} \tag{5}$$

being commonly accepted to consider this three terms formula for the inert fission gas modelling [33]. In the ANS 5.4–2010 methodology, the xenon diffusivity was revised to provide a better fit of the Halden Reactor Project release data, by assuming *a priori* values for the fuel surface-to-volume ratio. The revised xenon diffusivity, adopted in the ANS 5.4–2010 methodology, results in:

$$D = 7.6 \times 10^{-11}e^{-35000/T} + 1.41 \times 10^{-25}\sqrt{\dot{F}}e^{-13800/T} + 2 \times 10^{-40}\dot{F} \tag{6}$$

The diffusivities of other isotopes of interest are assumed to be equal or proportional to Eq. (6), i.e., $D(\text{Xe}) = D(\text{Kr}) = D(\text{I})$, based on experimental data [15,34].

The precursor enhancement factor α is a corrective factor to account for the observed increased diffusivity of some radioactive fission gas isotopes, based on the work of Friskney et al. [23]. The precursor enhancement factor α reproduces the effect of the first precursor (p) on the considered isotope (i). The effect of multiple precursors on the diffusivity is not considered. The relationship used in the current ANS-5.4-2010 methodology is:

$$\alpha = \left(\frac{1 - (y_0/x_0)^3}{1 - (y_0/x_0)^2}\right)^2 \tag{7}$$

where $y_0 = \sqrt{D_p/\lambda_p}$ and $x_0 = \sqrt{D_i/\lambda_i}$. λ_p and λ_i are the decay rates of the precursor and the considered isotope, respectively, and D_p and D_i are the intra-granular diffusivities of the precursor and the considered isotope, respectively. As a matter of fact, the release-to-birth ratio of an isotope significantly increases when its diffusion rate is slow relative to its precursor, especially when these have half-lives comparable with the irradiation time [23]. Intuitively, α reflects that the release-to-birth ratio of a daughter isotope is not exclusively determined by its own diffusivity. The fact that the precursor diffuses before the decay increases the release-to-birth ratio of the daughter isotope. This argument has been used to

explain the different release-to-birth ratios observed for [134]Cs and ^{137}Cs even though they should exhibit the same diffusivity [35]. Similarly, the difference in the observed release-to-birth ratios of [131]Xe and [132]Xe has been attributed to the diffusion of their precursors ^{131}I and [131]Te.

2.1.2. Inter-granular behaviour of radioactive fission gases

We report the ANS 5.4−2010 empirical-based description of the grain-boundary bubble interconnection process. The methodology exploits a modified version of the empirical Vitanza criterion, function of the local fuel temperature T (K) and burn-up β (MWd kgU^{-1}) [15,36]. Once the grain boundary interconnection has occurred, the ANS 5.4−2010 model assumes that the grain boundary remains linked to the rod internal free volume for the rest of the irradiation. The main assumptions considered in the ANS 5.4−2010 grain-boundary modelling are:

- Resintering of the grain boundary is neglected (once the fuel porosity is open, it remains open).
- Fuel densification is neglected.
- Grain sweeping mechanism (i.e., the accumulation of intra-granular gas at moving grain boundaries) is neglected.

The modifications implemented in the ANS 5.4−2010 model with respect to the Vitanza threshold are the following. The threshold is modified at burn-up values $\beta > 18.2$ MWd kgU^{-1}, to provide better agreement with Halden Reactor Project data about the release of radioactive fission gases of interest. In addition, the original threshold considered the fuel centerline temperature [36] while ANS 5.4 considers the local fuel temperature at a given radial node [15]). In the end, the calibration of the Vitanza threshold provides conservative estimations in the release-to-birth ratio evaluation.

The modified Vitanza threshold is grounded on the evaluation of a virtual interconnection temperature T_{IC}(K):

$$T_{IC}(K) = \frac{9800}{\ln(176\beta(\text{MWd kgU}^{-1}))} + 273 \qquad (8)$$

if β(MWd kgU^{-1}) < 18.2. Otherwise a linear decrease applies

$$T_{IC}(K) = 1434 - 12.85\beta(\text{MWd kgU}^{-1}) + 273 \qquad (9)$$

Then, the surface-to-volume ratio $S/V = 3/a$ (cm^{-1}) is chosen, depending on the local temperature T(K), during the irradiation:

$$\left(\frac{S}{V}\right) = 120 \text{ cm}^{-1}, \quad T < T_{IC} \qquad (10)$$

$$\left(\frac{S}{V}\right) = 650 \text{ cm}^{-1}, \quad T \geq T_{IC} \qquad (11)$$

when T_{IC} is attained, the release-to-birth ratio R/B is step-wisely increased, aiming to model the grain-boundary venting. The two given values of surface-to-volume ratio in Eqs. (10) and (11) result from experimental observation and are representative of the fuel surface-to-volume ratio [37]. The empirical nature of the ANS 5.4−2010 methodology is reflected in the capability to represent a selected set of radioactive fission gases released from UO$_2$ fuel with

densities between 95% and 98% of the theoretical density, with grain size between 6 μm to 15 μm and an open porosity between 0.1% and 3.0%[2] [15].

In the end, evaluating the R/B according to the ANS 5.4−2010 methodology can be summarized in these steps:

1. Evaluation of the local fuel burn-up β and of the interconnection temperature T_{IC} (Eqs. (8) and (9)).
2. Choice of the surface-to-volume ratio S/V, depending on whether $T \lessgtr T_{IC}$ (Eqs. (10) and (11)).
3. Computation of the local release-to-birth ratio R/B (Eq. (2)).

When performing an integral fuel rod simulation, where the whole rod is modelled with n radial and m axial nodes, the total R/B is determined by:

$$\left(\frac{R}{B}\right)_{\text{isotope}} = \sum_{j=1}^{m} \left(\frac{P_j^{\text{pellet}} V_j^{\text{node}}}{P^{\text{avg}} V^{\text{rod}}} \sum_{i=1}^{n} \frac{P_{i,j}^{\text{ring}} V_{i,j}^{\text{ring}}}{P_j^{\text{pellet}} V_j^{\text{node}}} \left(\frac{R}{B}\right)_{i,j} \right)$$
(12)

where P^{avg} is the average rod linear heat rate, P_j^{pellet} is the average linear heat rate of the pellet in the axial node j, $P_{i,j}^{\text{ring}}$ is the average linear heat rate of the local radial ring. The same notation holds for the volume variables.

2.2. Mechanistic modelling of radioactive fission gases

We provide an original mechanistic approach for modelling the radioactive fission gas behaviour. At the intra-granular level, we consider the time-dependent solution of Eq. (1). We get the solution exploiting Spectral Diffusion Algorithms (SDA), suitable also for fast transient conditions [14,39,40]. At the inter-granular level, we consider the physics-based modelling of inter-granular bubbles developed by Pastore and co-workers [13].

2.2.1. Intra-granular behaviour of radioactive fission gases

Considering a spherical fuel grain, the diffusion of radioactive fission gases towards the grain boundary is modelled with Eq. (1). Then, the concentration C (at m^{-3}) represents the residual amount of intra-granular fission gases. In our model we assume the same structure for the effective diffusivity, i.e., $D_{\text{eff}} = \alpha D$, adopted in ANS 5.4−2010, hence considering the correction due to the precursor effect by α (Eq. (7)). With respect to the ANS 5.4−2010 methodology, the formula that we consider for the intra-granular intra-granular diffusivity D is given by Eq (5), in line with the SCIANTIX validation for the modelling of inert gas behaviour [16]. In addition, by using Eq. (5) we avoid the additional ANS 5.4−2010 calibration of the diffusivity, outlined previously (Section 2.1.1).

In our model, we also consider the combined effect of trapping-in and irradiation-induced re-solution from intra-granular bubbles on the diffusivity [12,13,22,42] We apply the phenomenological model outlined by Speight [42] extended to account for radioactive isotopes, accordingly to the work of White et al. [22]. We assume that fission gas may be trapped at intra-granular gas bubbles at a rate g (s^{-1}). Conversely, the irradiation-induced re-solution from the bubbles back into the matrix occurs at a rate b (s^{-1}). The rates are calculated on the basis of the works of [43−45]. The rates, as well as the intra-granular bubble kinetics, are assumed to be independent of the considered precursor and we refer to Ref. [16] for their explicit formulation. The consequence of the trapping and resolution phenomena is that the total intra-granular concentration C is split into two separate contributions, $C = C_s + C_b$, being C_s the in-solution fission gas concentration (available for diffusion) and C_b

---

[2] The upper bound on the open porosity (i.e., 3.0%) is a remarkable large value for fuel with density between 95% and 98% of theoretical density [38]. When in the next section we will apply the ANS 5.4−2010 methodology to an irradiation condition of practical interest, this upper bound will be ensured.

the trapped fission gas concentration. Simultaneously, the decay process is considered and the following system of equations is obtained:

$$\begin{cases} \dfrac{\partial C_s}{\partial t} = \alpha D\nabla^2 C_s - \lambda C_s + bC_b - gC_s + B \\ \dfrac{\partial C_b}{\partial t} = gC_s - bC_b - \lambda C_b \end{cases} \tag{13}$$

By assuming the quasi-stationary condition $\partial C_b/\partial t = 0$, we replace Eq. (1) with:

$$\frac{\partial C}{\partial t} = D_{\text{eff}}\nabla^2 C - \lambda C + B \tag{14}$$

where the effective diffusion coefficient is

$$D_{\text{eff}} = \frac{b + \lambda}{b + \lambda + g}\alpha D \tag{15}$$

In the end, this approach results in a simple modification of the effective diffusion coefficient and can be effectively implemented in the solution of the original diffusion-decay equation (Eq. (1)).

From the numerical point of view, the intra-granular diffusion-decay equation (Eq. (1)) is solved with a spectral diffusion algorithm [39,40], currently implemented in SCIANTIX. The numerical solver is verified with the method of the manufactured solutions [46] and an extensive error analysis has been developed in a separate work by the authors [14]. The numerical solver for Eq. (1) provides time-dependent evolution of the intra-granular concentration C, hence of the release-to-birth ratio R/B, and removes the secular equilibrium hypothesis (Section 2.1.1). With respect to the ANS 5.4–2010 solution, we solve Eq. (1) in a spherical grain of physical size. In other words, we consider an equivalent radius that is coherent with the real fuel grain dimension $a \approx 5~\mu$m, avoiding imposing an *a priori* S/V.

2.2.2. Inter-granular behaviour of radioactive fission gases

Modelling the inter-granular bubble kinetics impacts the release of fission gas in the fuel rod free volume and the fuel pellet swelling. The inter-granular behaviour of short-lived fission gases is modelled with the same physics-based approach, already implemented in SCIANTIX for the stable fission gas behaviour, that is the description given in the work of Pastore and co-workers [13]. We assume that the grain-boundary venting is mainly driven by stable fission gas and that short-lived fission gases, negligible in mass with respect to stable isotopes, are not relevant in determining grain-boundary venting.[3] Inter-granular bubbles develop on the grain boundaries and continuously absorb fission gas released from the grain matrix. Bubbles grow and coalesce on the grain boundaries until their saturation takes place, leading to the formation of a pathway connected with the pellet surface. Then, fission gas percolates through the open porosity and is released to the fuel rod free volume [13,22,24]. The grain-boundary saturation process represents an incubation time for the onset of the thermal release [36]. The delay is caused by the initially closed porosity of the fuel

microstructure. In the case of short-lived radioactive fission gases, this delay is significant. Hence, suitable modelling of this incubation period is required. From the modelling point of view, the grain-boundary behaviour is described with the capillarity relation. Over-pressurized bubbles tend to return to the equilibrium state by absorbing vacancies beyond gas atoms, growing in size until coalescence takes place [13,22,24]. The mechanical equilibrium pressure is given by Refs. [13,24,47,48]:

$$p_{\text{eq}} = \frac{2\gamma}{R_{\text{gf}}} + \sigma_h \tag{16}$$

The term $2\gamma/R_{\text{gf}}$ (Jm^{-3}) is the Laplace pressure, with γ (Jm^{-2}) surface tension of the bubble and R_{gf} curvature radius, σ_h is the hydrostatic stress (here negative for a medium under compression). The surface tension γ differs from the UO$_2$/UO$_2$ interface one, consequently the geometrical form of the lenticular bubbles has a semi-dihedral angle $\theta \approx 50°$ [49]. The absorption of vacancies is the main cause of grain boundary bubble growth and shrinkage [42]. The vacancy absorption/emission rate is given by

$$\frac{dn_v}{dt} = \frac{2\pi D_v \delta_g}{k_B TS}(p - p_{\text{eq}}) \tag{17}$$

where S is calculated as

$$S = \frac{-((3 - F_c)(1 - F_c) + 2\ln F_c)}{4} \tag{18}$$

According to Refs. [13,24], the gas pressure in the bubble is written as $p = kTn_g/\Omega_{\text{fg}}n_v$. We pose the volume of a grain-face bubble given by the summation of fission gas atoms and vacancies, evaluating the bubble volume as[4] $V_{\text{gf}} = n_g\omega + n_v\Omega_{\text{gf}}$. By assuming a bubble of circular projection, the radius of the bubble is given by:

$$R_{\text{gf}} = \left(\frac{3V_{\text{gf}}}{4\pi\phi(\theta)}\right)^{1/3} \tag{19}$$

where $\phi(\theta) = 1 - 1.5\cos\theta + 0.5\cos^2\theta$. The mechanistic approach exploited for the grain-boundary bubble coalescence is described in earlier works [13,24,26] and results in the following equation for the evolution of the number of grain-boundary bubbles N_{gf} (bub m^{-2}):

$$\frac{dN_{\text{gf}}}{dA_{\text{gf}}} = -2\,N_{\text{gf}}^2 \tag{20}$$

where the projected area of the grain-boundary bubble is $A_{\text{gf}} = \pi(R_{\text{gf}}\sin\theta)^2$. All the SCIANTIX modelling parameters are available in Table 3.

Fission gas release, from grain-face bubbles to the fuel rod free volume, is mainly a consequence of the gas venting from the grain faces. We account for this process through the grain-boundary saturation, namely, when the coverage reaches the saturation

---

[3] This approximation is valid in stationary conditions, at the radioactive equilibrium of the considered isotopes. In this condition, the amount of radioactive isotopes is in proportion negligible with respect to the stable isotopes. Nevertheless, given the list of short-lived fission gases modelled with SCIANTIX (See Table 5), the radioactive equilibrium is achieved for most of the isotopes also during short irradiation periods of engineering interest (power transients characterised by few hours of holding time). On top of that, the approximation validity is reinforced because the fission yield of radioactive fission gases is lower than the fission yield of stable fission gases.

---

[4] In this work, the application of $V_{\text{gf}} = n_g\omega + n_v\Omega_{\text{gf}}$ is limited to the grain boundary region. The existence of various types of grain boundaries (e.g. with varying degrees of misalignment of adjacent grains [50]), atomistic-scale calculations of grain boundary defects and their interaction with fission products in ionic ceramic fuels, have not yet attained the same level of maturity as those in the bulk materials [51–54]. That is in part due to the inherent complex structure of grain boundaries in ionic crystals, which are generally assumed to contain more vacancies that can promote diffusion/trapping of fission products. Therefore, we adopt this simplified approach, that allows the calculation of the bubble growth rate from the combined effects of the inflow of atoms (from the intra-granular region) and the absorption/emission of vacancies in the bubble.

Table 3
List of the parameters used in the SCIANTIX modelling for radioactive fission gas behaviour [16].

Symbol	Definition/value	u.o.m.	Reference
λ	Decay rate	s^{-1}	
y	Fission yield	at $fiss^{-1}$	
a	Grain radius	m	
α	Precursor enhancement factor	(−)	[15, 23]
D	Single-atom diffusivity in UO_2	$m^2 s^{-1}$	[32]
	$D_1 + D_2 + D_3$		
	$D_1 = 7.6e - 10 \exp(-4.86e - 19/k_B T)$		
	$D_2 = 5.64e - 25\sqrt{\dot{F}}\exp(-1.91e - 19/k_B T)$		
	$D_3 = 2e - 40\dot{F}$		
	$\dot{F}$ (fiss $m^{-3} s^{-1}$), fission rate density		
	T (K), local fuel temperature		
	k_B (JK^{-1}), Boltzmann constant		
D_v	vacancy diffusivity in grain boundary	$m^2 s^{-1}$	[59]
	$D_v = 6.9e - 4 \exp(-5.35e - 19/k_B T)\, m^2 s^{-1}$		
$F_{c, sat}$	saturation fractional coverage	(−)	[26, 24]
	$F_{c, sat} = 0.5$		
γ	UO_2 gas specific surface energy	(Jm^2)	[59]
δ_g	thickness of the diffusion layer at grain boundary	(m)	[59]
	$\delta_g = 5e - 10\, m$		
θ	semi-dihedral angle	(°)	[24]
	$\theta = 50°$		
ω	Van der Waal's volume of a fission gas atom	(m^3)	[13]
	$\omega = 8.25e - 29\, m^3$		
Ω_{gf}	vacancy volume in grain-face bubble	(m^3)	[59]
	$\Omega_{gf} = 4.09e - 29\, m^3$		

value $F_{c, sat} = 0.5$ [13,24,26] a fraction of the gas within grain-face bubbles is released, to compensate for further bubbles growth and maintain $dF_c/dt = 0$. Moreover, in addition to the thermal fission gas release, it is known from experimental observations that fission gas release can occur after grain-face separation due to micro-cracking [55−57]. The model for burst fission gas release associated with fuel micro-cracking accounts for the experimental observation and, when it is considered during simulations, the saturation fractional coverage $F_{c, sat}$ is subjected to variations in its value [58]. In particular, the micro-cracking effect consists in a reduction of the fission gas storing capability of the grain boundary, represented by a change of the saturation fractional coverage, and in a partial release of the grain-boundary gas, represented by a change of the fractional coverage [58]. When the saturation threshold $F_{c, sat}$ is reached, the instantaneous release is assumed to occur, i.e., fission gas is brought from the grain boundaries to the fuel rod free volume. We neglect all the mechanisms that intervene while fission gas is transported from the grain boundary to the fuel rod free volume, e.g. long-distance axial transfer, percolation, grain-face diffusion. The neglected phenomena are assumed to not considerably affect the amount of released isotopes [25]. We assume that this argument holds both for stable and radioactive fission gas atoms.

In order to evaluate the fraction of radioactive fission gas released from the fuel, we need to compute the total amount of decayed fission gas, in particular, the concentration of radioactive fission gas embedded on the grain boundaries C_b (at m^{-3}) results from the following equation:

$$\frac{dC_b}{dt} = -\left(\frac{3}{a}D_{\text{eff}}\frac{\partial C}{\partial r}\right)_{r=a} - \lambda C_b - R \qquad (21)$$

The release rate R (at $m^{-3} s^{-1}$) accounts for the fission gas atoms, embedded on grain boundaries, that are released to the fuel rod free volume as soon as the grain-boundary venting occurs. A summary of the inter-granular part of the SCIANTIX modelling of radioactive fission gas behaviour is provided in what follows. We assume that grain boundaries are populated with an initial number

of bubbles (one-off nucleation [24]). Fission gas atoms diffuse from within the grain to the grain boundaries and are collected in inter-granular bubbles. We assume that atoms on the grain boundaries exist only within bubbles. We neglect re-solution events from the grain-face bubbles back to the fuel grains. Lastly, grain-edge bubbles are not considered. Fission gas is continuously collected in grain-boundary bubbles, while bubble growth and coalescence occur. Bubble growth is treated considering the vacancy-controlled diffusion and absorption phenomena [13,48]. The mechanism that drives bubble interconnection is bubble coalescence, modelled with Eq. (20) [24]. The onset of fission gas release is given by the grain-face saturation [13,25]. Once the saturation condition is attained, we assume that further bubble growth is balanced by bubble loss and fission gas release[5] in order to maintain $dF_c/dt = 0$.

3. Model testing as standalone version

The model herein developed (Section 2.2) has been integrated into the current version of SCIANTIX, a multi-scale code tailored for fission gas behaviour modelling [16]. As a first application, we use SCIANTIX as a standalone module to simulate a CONTACT experiment [60,61].

3.1. Description of the CONTACT 1 experiment

The CONTACT experiments were part of a cooperative project among CEA and FRAMATOME on the behaviour of PWR fuel rods at constant power. The tests took place in the SILOE reactor and involved an in-pile study of short fuel rods composed of UO_2 pellets wrapped in a Zr-4 cladding. The fuel rods involved were named CONTACT 1, 2, 2-bis and 3. We focus on the CONTACT 1 - FRAMATOME rodlet since this case is dominated by diffusional release,

---

[5] From the point of view of the numerical code, the fission gas stored in the grain boundary is not divided into two separate "unvented bubbles" and "vented bubbles" contributions. At each time step, the fractional coverage is monitored and as soon as the saturation value is attained, a part of the fission gas stored at the grain boundary is released (to restore the saturation value).

whereas the other experiments are performed at lower power and burn-up and thus dominated by athermal release, which is not (yet) considered in the SCIANTIX code.

The pellet stack was thermally isolated at both ends by aluminia oxide pellets (Al_2O_3) and an inconel spring ensured its axial holding. The capsule was located in a PWR loop, at 13 MPa (to best represent the effect of the cladding creep down) and the nucleate boiling regime provided an external cladding temperature of 330 °C. The linear power, the fuel centerline temperature (FCLT), the cladding outer diameter at power, the release of stable inert fission gases and the release-to-birth ratios for some short-lived fission gases (between ^{133}Xe and ^{89}Kr) were measured [60,61]. The scheme of the device and the instrumentation is shown in Fig. 1. The linear power was measured by six self-powered rhodium neutron detectors and the calibration curves reported a 3% of accuracy. To measure the FCLT a 1.5 mm diameter central hole was drilled in the pellets to accommodate the thermocouple (Fig. 1). The measured R/B values at low burn-up, namely prior to grain-boundary venting, spans over one order of magnitude, from 1e-4 to 1e-3. Such values may be ascribed to several non-diffusional release mechanisms by recoil, fuel cracking and micro-cracking [60], together with the increase of S/V due to the central hole. In accordance with previous work [62] the release-to-birth ratio of short-lived fission gases swept by carrier gas may appear also higher due to the central hole contribution where the temperature is higher, especially at low burn-up ($R/B \approx 3e-4$ against the $R/B \approx 4e-5$ from solid pellets [62,63]).

The devices were located in such an area of the PWR loop where the neutron flux was uniform and the axial power variations were negligible, i.e., less than 2% [61]. The CONTACT 1 device was irradiated at a constant linear rating close to 40 kWm^{-1}. The CONTACT 1 experiment began in September 1978 and ended in July 1980 and each irradiation cycle consisted of 21 days of irradiation per month. The experiment got interrupted from April to September 1979 due to an accidental introduction of air into the water loop. After this event, a 30 μm layer of oxide has been detected on the surface of the cladding. Moreover, in September 1979 the composition of the filling gas has been changed from 1 MPa of He to 0.1 MPa of Ne, and then the irradiation continued up to approximately 22 MWd kgU^{-1}.

The adopted FRAMATOME fuel pellets were characterized by a surface-to-volume ratio of 50 cm^{-1} [61]. Other details of the rodlet are collected in Table 4.

The results of CONTACT 1 concerns the evolution of the FCLT, the cladding diameter, the fractional release of stable fission gas (obtained through the measurement of the long-lived ^{85}Kr isotope) and the release-to-birth ratio of short-lived fission gases. The monitored short-lived fission gases are given in Table 5. In particular, our objective is to use the previously developed model (Section 2.2), implemented in the standalone SCIANTIX version, to compute the evolution of release-to-birth ratios (R/B) for the short-lived fission gases listed in Table 5 and the results are presented in the following section. Within the CONTACT experimental reports, there is not a precise indication for the experimental R/B uncertainty. Moreover, the behaviour of the measured points at the beginning and at the end of the irradiation is suspicious (Fig. 5). For example, the fact that at the end of the irradiation some points increase while others decrease could not be entirely a consequence of the different half-lives of the isotopes and could be an indication of the measurement uncertainty. On top of that, because of the lack of an accepted deviation between the calculated and measured release-to-birth ratio, that could take into account inherent modelling uncertainty, according to the ANS 5.4–2010 report [15] we extrapolated an uncertainty band on the measured R/B for both short-lived xenon and krypton fission gases of about a factor of 5, that we apply in our next analysis.

In addition, the ^{133}Xe measurement at 10 MWd kgU^{-1} shows an unusual increase after the extended shut-down of the reactor (from April to September 1979). Due to a lack of details regarding this incident, it is not clear if the mentioned ^{133}Xe measured point can be ascribed to instrumentation errors, even if it seems the most reasonable explanation. In any case, this point must be cautiously considered.

3.2. Simulations of the CONTACT 1 experiment

To simulate the CONTACT 1 rodlet, SCIANTIX requires as input quantities the fuel temperature T (K), the fission rate density F (fiss m^{-3} s^{-1}) and the fuel hydrostatic stress σ_h (MPa). We obtained the required initial conditions (see Figs. 2–4) from the TRANSURANUS code [6,7], for which the adequate CONTACT 1 input file is available. We adopt the average fuel temperature, computed by TRANSURANUS (Fig. 2). Indeed SCIANTIX, being a 0D multi-scale code, operates with a local time-dependent temperature provided
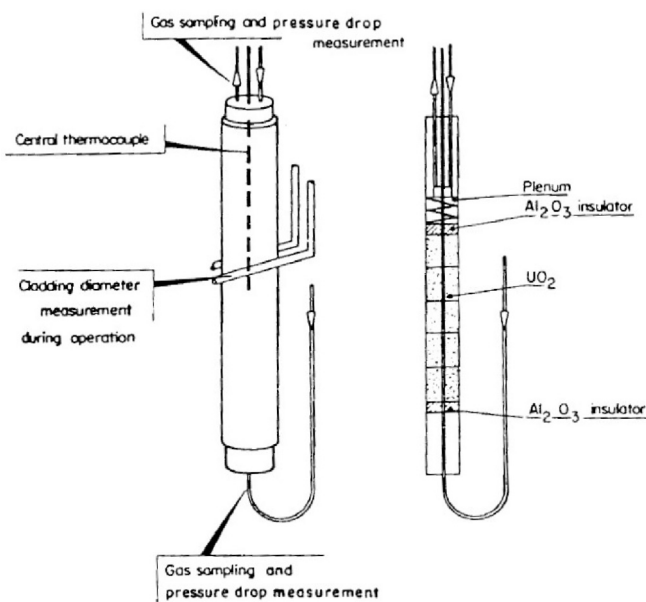

Fig. 1. Scheme of the experimental capsule with the FRAMATOME fuel rod and instrumentation used in CONTACT 1 experiments [61].

Table 4
Specifications of the short fuel rod used in the CONTACT 1 - FRAMATOME (C 1) experiment [61].

	Parameter	Units	C 1
Pellets	Length	mm	14
	Diameter	mm	8.19
	Dish dept	mm	0.13
	Dish radius	mm	14.73
Cladding	Internal diameter	mm	8.36
Cladding	External diameter	mm	9.50
Plenum	Length	mm	7.7
Fuel column	Number of pellets		5
	Enrichment	%	4.95
	Geometric density	% TD	95
Irradiation	Nominal rating	kWm^{-1}	40.5
	Peak rating	kWm^{-1}	41
	Average rating	kWm^{-1}	36
	Fast flux ($E > 1$ MeV)	nm^{-2} s^{-1}	6.5×17
	Discharge burn-up	MWd kgU^{-1}	22
	Clad ext. temperature	°C	330
Loop pressure		MPa	13

Table 5
List of the short-lived fission gases, together with their half-lives, for which the release-to-birth ratio was measured during the CONTACT 1 experiment [61].

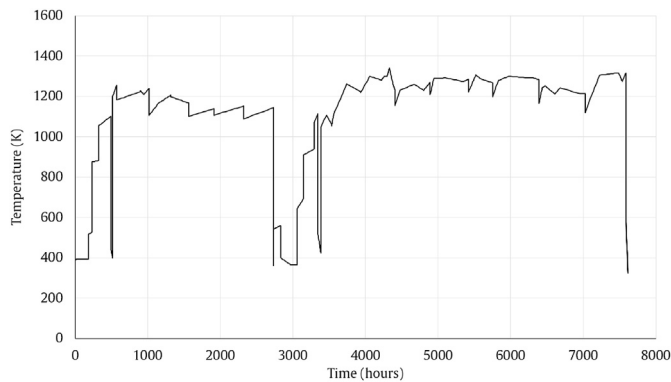| Isotope	Half-life
^{133}Xe	5.29 d
^{135m}Xe	15.7 min
^{135}Xe	9.16 h
^{137}Xe	3.8 min
^{138}Xe	14.13 min
^{85m}Kr	4.48 h
^{87}Kr	76.4 min
^{88}Kr	2.86 h
^{89}Kr	3.18 min

Fig. 2. Average fuel temperature T (K), computed with TRANSURANUS, used as input for the SCIANTIX simulation.
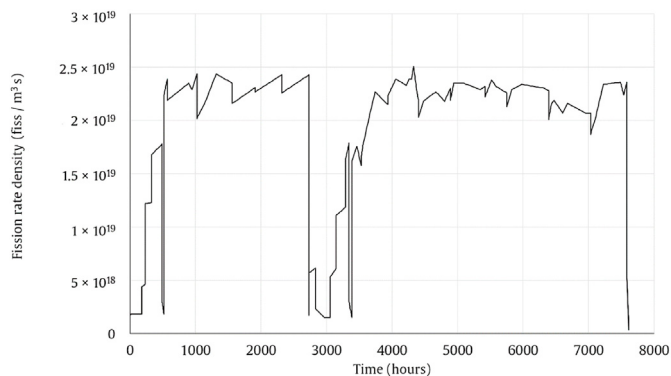
Fig. 3. Fission rate density F (fiss m^{-3} s^{-1}), computed with TRANSURANUS, used as input for the SCIANTIX simulation.

Fig. 4. Radially averaged hydrostatic stress (> 0, compressive) in the fuel σ_h (MPa) for the SCIANTIX simulation, derived from TRANSURANUS.

as input, and not with a time-dependent radial profile. The most representative temperature for the simulation of all the fuel stack hence is the average fuel temperature. Indeed, considering a radial temperature profile would affect mostly the thermal release onset (because of the presence of a hotter zone) without significantly variations in the asymptotic R/B of the isotopes (because higher release from the hotter part would be balanced by the lower release from the colder part, and the average temperature that we use is a good representation of the average thermal behaviour of the fuel). A similar argument holds for the input hydrostatic stress. Namely, the radial average of the hydrostatic stress in a fuel slice is computed from TRANURANUS (see Fig. 4) and becomes a SCIANTIX

input. From the following discussion of the results, it is verified that the used average input values are an acceptable "0D" representation of the CONTACT 1 experiment.

In addition, the fuel design characteristics for the CONTACT 1 case are given in Table 4. The initial size of the fuel grains is not given [61] but according to a 2002 review of the IFPE documents, a grain diameter of about 6–8 μm is consistent with the fuel microstructure. In line with the TRANSURANUS input file, we set the initial grain radius to 5 μm (needed for the SCIANTIX simulation) but a certain level of uncertainty must be taken into account.

3.2.1. CONTACT 1: SCIANTIX prediction

By using the presented radioactive fission gas model (Section 2.2), we computed the release-to-birth ratios (R/B) for the short-lived fission gases between ^{133}Xe and ^{89}Kr, namely the ones for which data are given, and we compare our predictions with the experimental measurements provided by the online gamma detectors (Fig. 5).

First, since all the available experimental data are given as a function of the burn-up, we show the burn-up predicted by SCIANTIX against the measured burn-up (Fig. 6). The agreement is acceptable, with a relative error on the final value of 1.5% and on the integral average of about 5%, confirming the soundness of the extracted input history and allowing us to compare our predicted results with the experimental measurements as a function of the burn-up. We also report the predicted (stable) fission gas release against the measured one. The data for the fission gas release is obtained by measuring the long-lived ^{85}Kr (which has a half-life of about 10.7 years).

Performing a 0D simulation of the rodlet impacts the difference in the predicted thermal release onset (≈ 7.7 MWd kgU^{-1}) against the experimental evidence (≈ 2.5 MWd kgU^{-1}) (Fig. 7). The predicted fission gas release before the thermal onset is due to the micro-cracking model, described in detail in the work of Barani and co-workers [64], that we extend to the radioactive fission gases.

Concerning the release of the short-lived fission gases, studied in this work via the release-to-birth ratio, our prediction is shown in Fig. 8. As for the stable fission gas release (Fig. 7), we predict a first release contribution due to the temperature transients activating the micro-cracking model, then a second release contribution driven by the grain-boundary venting. With reference to the intra-granular diffusion-decay process, we treat all the isotopes in the same way. Namely, we assume the same effective diffusivity D for both xenon and krypton isotopes (i.e. we consider the intra-granular trapping and re-solution phenomena to be in equilibrium)
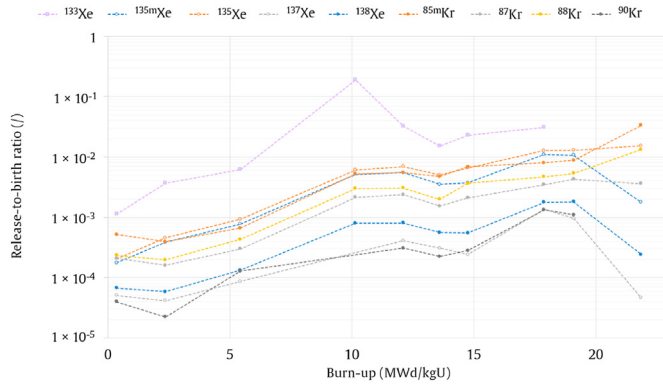
Fig. 5. Release-to-birth ratios (R/B) of short-lived fission gases, measured during the CONTACT 1 - FRAMATOME experiment, as a function of the burn-up (MWd kgU^{-1}).
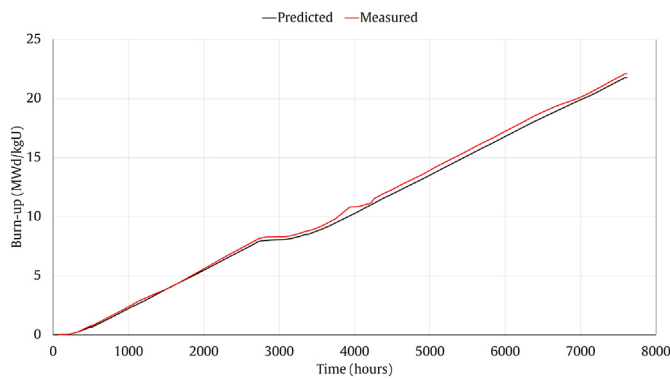

Fig. 8. Release-to-birth ratios (R/B) of the short-lived fission gases predicted by the SCIANTIX, as a function of the burn-up (MWd kgU^{-1}). The predicted R/B increases as soon as the grain-boundary venting occurs, in line with our mechanistic description.

Fig. 6. Comparison between the measured burn-up and the predicted one.

Fig. 7. Comparison between the measured fission gas release (via the long-lived ^{85}Kr) and the predicted one.

considering this performance indicator we observe that our predictions are quantitatively in agreement with the ANS 5.4–2010 methodology.

3.2.2. CONTACT 1: application of the ANS 5.4–2010 methodology

Since the ANS 5.4–2010 methodology is validated and tailored to reproduce stationary PWR reactor operation, we use it as a state-of-the-art reference to estimate the release-to-birth ratios of the available short-lived fission gases. Namely, the ones that are included in the spectrum from krypton 89 to xenon 133. Thanks to the previous ANS 5.4–2010 definition of the equilibrium release-to-birth ratio R/B (Eq. (2)) it is indeed possible to estimate the release-to-birth ratios measured during the CONTACT experiments. We exploit the version of the ANS 5.4–2010 methodology recently implemented in TRANSURANUS to evaluate the R/B of interest and we compare the results both with our predictions (Fig. 8) and with the experimental data (Fig. 5). The comparison is carried for the short-lived fission gas isotopes for which we have both experimental data and ANS 5.4–2010 R/B estimation, i.e., ^{85m}Kr, ^{133}Xe, ^{135}Xe, ^{135m}Xe, ^{88}Kr and ^{87}Kr. We show the results in Figs. 9–14. We compute the root mean square error of the release-to-birth ratios predicted by both our mechanistic model and by the ANS 5.4–2010 methodology, and we show the results in Table 6.

We highlight in what follows some peculiar aspects emerging from the comparison of the simulation results with the experimental data in Figs. 9 - 14.

1. By using the average fuel temperature for the simulation we obtain a satisfactory agreement on the release-to-birth ratio evolution in time, once the grain-boundary venting occurs. Before the grain-boundary venting (that occurs at about 7.7 MWd kgU^{-1}, according to our model) the release from the fuel is dominated by athermal processes, considered in the present work only through the micro-cracking model.
2. Our mechanistic model is developed within the SCIANTIX environment, built upon the use of physics-based models, when available [16]. Fuel design parameters, such as the grain radius a, hence assume initial values as representative as possible of the physical value, are time-dependent quantities that evolve during the irradiation and influence the overall set of SCIANTIX models. Similarly, the default intra-granular diffusivity D for stable fission gases (xenon and krypton) is expressed by Eq. (5) and we assume the same diffusivity for long- and short-lived isotopes of xenon and krypton. In the end, by avoiding any kind of artificial tuning and using parameters that are physically

but we account for the precursor effect via the corrective factor α (Eq. (7)). These assumptions are in line with the ANS 5.4–2010 methodology [15]. Accordingly, the release kinetics of the different species has the same shape and the difference in the absolute value is a consequence of the different α and λ of each isotope. The predicted R/B are in qualitative agreement with the experimental data, by showing also a coherent increase with the burn-up. The values are enclosed in the aforementioned uncertainty band that we estimated from the ANS 5.4–2010 report [15]. With respect to the available R/B experimental points (Fig. 5), we compute the burn-up mean square error (Table 6). As we describe in the next section, by
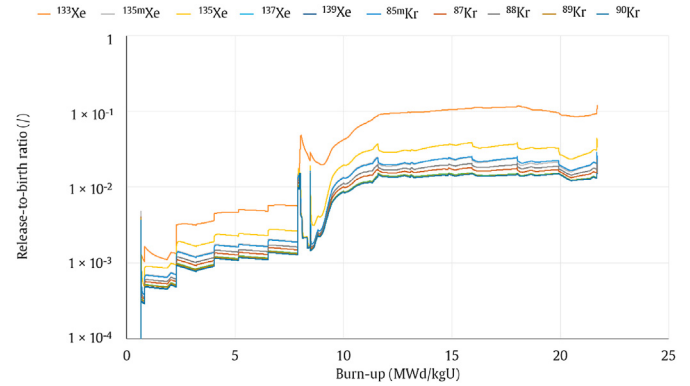
Table 6
Root mean square error of release-to-birth ratios with respect to the experimental data, for the developed mechanistic model and the semi-empirical ANS 5.4–2010 methodology.

Isotope	RMSE - ANS 5.4–2010	RMSE - SCIANTIX
^{133}Xe	4.57×10^{-3}	5.28×10^{-3}
^{135m}Xe	2.10×10^{-5}	1.60×10^{-4}
^{135}Xe	5.37×10^{-5}	3.55×10^{-4}
^{85m}Kr	1.27×10^{-4}	1.50×10^{-4}
^{87}Kr	3.86×10^{-6}	1.15×10^{-4}
^{88}Kr	4.57×10^{-3}	5.28×10^{-3}
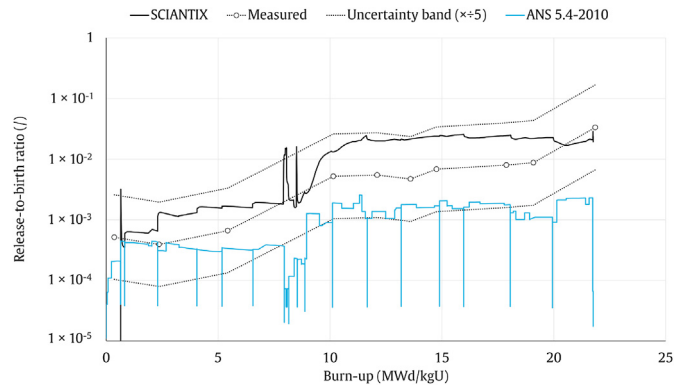
Fig. 9. ^{85m}Kr: comparison of the release-to-birth ratio measured during the CONTACT 1 - FRAMATOME experiment against the SCIANTIX mechanistic prediction and the semi-empirical evaluation of the ANS 5.4–2010 methodology.
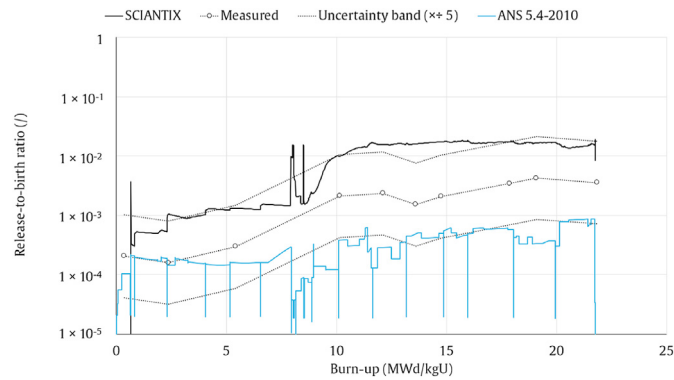
Fig. 10. ^{87}Kr: comparison of the release-to-birth ratio measured during the CONTACT 1 - FRAMATOME experiment against the SCIANTIX mechanistic prediction and the semi-empirical evaluation of the ANS 5.4–2010 methodology.

Fig. 11. ^{88}Kr: comparison of the release-to-birth ratio measured during the CONTACT 1 - FRAMATOME experiment against the SCIANTIX mechanistic prediction and the semi-empirical evaluation of the ANS 5.4–2010 methodology.

Fig. 12. ^{133}Xe: comparison of the release-to-birth ratio measured during the CONTACT 1 - FRAMATOME experiment against the SCIANTIX mechanistic prediction and the semi-empirical evaluation of the ANS 5.4–2010 methodology.

Fig. 13. ^{135}Xe: comparison of the release-to-birth ratio measured during the CONTACT 1 - FRAMATOME experiment against the SCIANTIX mechanistic prediction and the semi-empirical evaluation of the ANS 5.4–2010 methodology.

significant, we obtain time-dependent predictions that are in agreement with the experimental data.

3. The semi-empirical ANS 5.4–2010 methodology considers two artificially tuned quantities in the computation of the release-to-birth ratios, namely the intra-granular diffusivity D and the surface-to-volume ratio S/V, which corresponds to the idealized (i.e. nonphysical) grain size. The former is reduced by one order of magnitude in the intrinsic component and by a factor of four in the vacancy-assisted diffusivity, the latter decreased with respect to the surface-to-volume ratio of a physical UO_2 grain, since it aims to represent the surface-to-volume ratio of the whole fuel pellet. Due to these manipulations, it could appear logical that the predicted R/B values underestimate the measured ones.
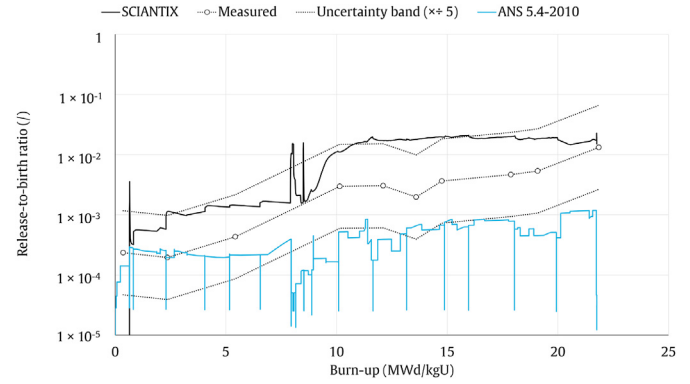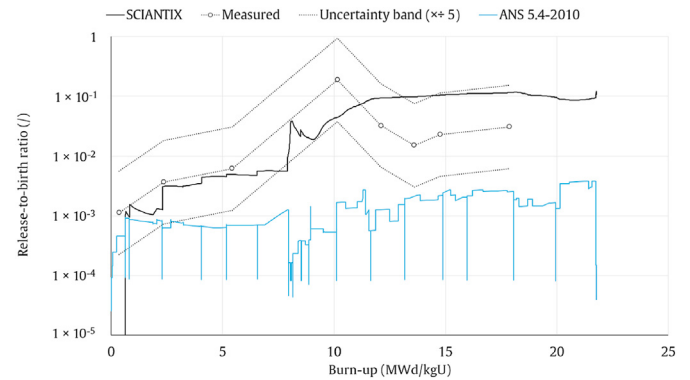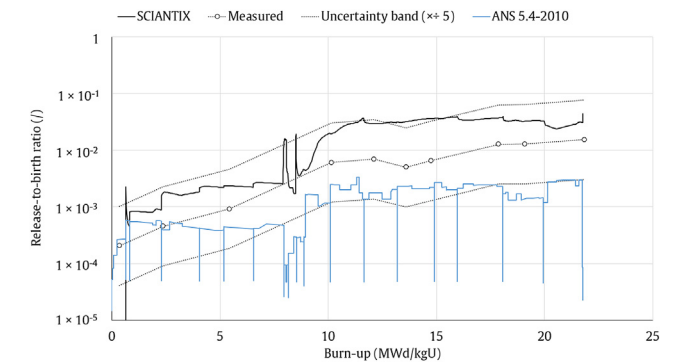
4. Conclusions

In the present work, we developed a model for evaluating the release-to-birth ratios of short-lived fission gases (namely, short-lived isotopes of xenon and krypton). The model starts from the ANS 5.4–2010 intra-granular description of the transport of these fission gases towards the grain boundaries. The ANS 5.4–2010 methodology is a semi-empirical methodology tailored to evaluate the release-to-birth ratio of short-lived radioactive fission gases
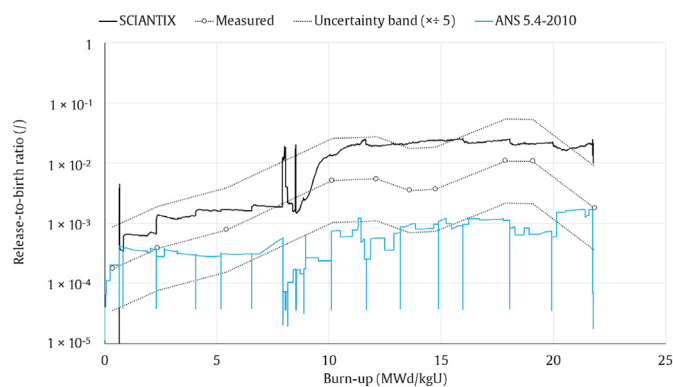
Fig. 14. ^{135m}Xe: comparison of the release-to-birth ratio measured during the CON-TACT 1 - FRAMATOME experiment against the SCIANTIX mechanistic prediction and the semi-empirical evaluation of the ANS 5.4–2010 methodology.

and volatile fission products. The main assumptions of the methodology are the secular equilibrium hypothesis and empirical description of the grain-boundary venting, together with the artificial tuning of the fuel pellet surface-to-volume ratio (prior to and after the grain-boundary venting) and the intra-granular diffusivity of the fission gas. We solve the intra-granular diffusion-decay problem numerically with a spectral diffusion algorithm. Then, the inter-granular description is improved by taking into account the radioactive decay of the fission gases, during the grain-boundary bubble growth, coalescence and interconnection processes, which ultimately give rise to the so-called grain-boundary venting and constitute the release onset. With regard to the inter-granular description, we assume that the radioactive fission gases of primary interest are negligible in mass with respect to the stable ones, therefore not significant in determining the grain-boundary venting process. The developed model is integrated into SCIANTIX, a 0D grain-scale code tailored for inert fission gas behaviour modelling. We compute the time-dependent fractional release for a set of short-lived fission gases, and we compare our predictions with the experimental measurements available from the CONTACT 1 experiment, and against the ANS 5.4–2010 modelling available through the TRANSURANUS fuel performance code. The predictions of our model are in satisfactory agreement with the experimental data and in most cases at least as good as the ANS 5.4–2010 predictions.

The SCIANTIX model shows its capability in handling in an effective way the numerical solution of the diffusion-decay problem, also for the short-lived fission gases characterised by a half-live of the order of magnitude of the minutes. A second work will follow the present one, providing further integral fuel rod analysis by coupling the current model with the thermo-mechanical code TRANSURANUS.

Declaration of competing interest

The authors declare that they have no known competing financial interests or personal relationships that could have appeared to influence the work reported in this paper.

Acknowledgements

References

[1] G. Ducros, P.P. Malgouyres, M. Kissane, D. Boulaud, M. Durin, Fission product release under severe accidental conditions: general presentation of the program and synthesis of VERCORS 1-6 results, Nucl. Eng. Des. 208 (2) (2001) 191–203, https://doi.org/10.1016/S0029-5493(01)00376-4.

[2] J.H. Song, S.M. An, T. Kim, K.S. Ha, Post-Fukushima challenges for the mitigation of severe accident consequences, Nucl. Eng. Technol. 52 (11) (2020) 2511–2521, https://doi.org/10.1016/j.net.2020.04.031.

[3] K. Tagami, S. Uchida, N. Ishii, J. Zheng, Estimation of Te-132 distribution in fukushima prefecture at the early stage of the Fukushima Daiichi Nuclear Power Plant reactor failures, Environ. Sci. Technol. 47 (10) (2013) 5007–5012, https://doi.org/10.1021/es304730b.

[4] R.S. Denning, R.J. Budnitz, Impact of probabilistic risk assessment and severe accident research in reducing reactor risk, Prog. Nucl. Energy 102 (2018) 90–102, https://doi.org/10.1016/j.pnucene.2017.05.021.

[5] R2CA, URL, http://r2ca-h2020.eu.

[6] A. Magni, A.D. Nevo, L. Luzzi, D. Rozzia, M. Adorni, A. Schubert, P. Van Uffelen, The TRANSURANUS fuel performance code, in: J. Wang, X. Li, C. Allison, J. Hohorst (Eds.), Nuclear Power Plant Design and Analysis Codes - Development, Validation and Application, Woodhead Publishing Series in Energy, Elsevier, 2021, pp. 161–205. Ch. 8.

[7] K. Lassmann, TRANSURANUS: a fuel rod analysis code ready for use, Nucl. Mater. Fission React. (1992) 295–302, https://doi.org/10.1016/b978-0-444-89571-4.50046-3.

[8] B. Dong, L. Li, C. Li, W. Zhou, J. Yin, D. Wang, Review on models to evaluate coolant activity under fuel defect condition in PWR, Ann. Nucl. Energy 124 (2019) 223–233, https://doi.org/10.1016/j.anucene.2018.10.009.

[9] B.J. Lewis, P.K. Chan, A. El-Jaby, F.C. Iglesias, A. Fitchett, Fission product release modelling for application of fuel-failure monitoring and detection - an overview, J. Nucl. Mater. 489 (2017) 64–83, https://doi.org/10.1016/j.jnucmat.2017.03.037.

[10] L.E. Herranz, L. Lebel, F. Mascari, C. Spengler, Progress in modeling incontainment source term with ASTEC-Na, Ann. Nucl. Energy 112 (2018) 84–93, https://doi.org/10.1016/j.anucene.2017.09.037.

[11] S. Nichenko, J. Kalilainen, L. Fernandez Moguel, T. Lind, Modelling of fission products release in VERDON-1 experiment with cGEMS: coupling of severe accident code MELCOR with GEMS thermodynamic modelling package, Ann. Nucl. Energy 152 (2021) 107972, https://doi.org/10.1016/j.anucene.2020.107972.

[12] D. Pizzocri, G. Pastore, T. Barani, A. Magni, L. Luzzi, P. Van Uffelen, S.A. Pitts, A. Alfonsi, J.D. Hales, A model describing intra-granular fission gas behaviour in oxide fuel for advanced engineering tools, J. Nucl. Mater. 502 (2018) 323–330, https://doi.org/10.1016/j.jnucmat.2018.02.024.

[13] G. Pastore, L. Luzzi, V. Di Marcello, P. Van Uffelen, Physics-based modelling of fission gas swelling and release in UO$_2$ applied to integral fuel rod analysis, Nucl. Eng. Des. 256 (2013) 75–86, https://doi.org/10.1016/j.nucengdes.2012.12.002. https://linkinghub.elsevier.com/retrieve/pii/S0029549312005754.

[14] G. Zullo, D. Pizzocri, L. Luzzi, On the use of spectral algorithms for the prediction of short-lived volatile fission product release: Methodology for bounding numerical error, Nuclear Engineering and Technology https://doi.org/10.1016/J.NET.2021.10.028. URL https://linkinghub.elsevier.com/retrieve/pii/S1738573321006148.

[15] J.A. Turnbull, C.E. Beyer, in: Background and Derivation of ANS-5.4 Standard Fission Product Release Model, United States Nuclear Regulatory Commision, 2010, p. 11. URL, http://www.nrc.gov/reading-rm.html.

[16] D. Pizzocri, T. Barani, L. Luzzi, SCIANTIX: a new open source multi-scale code for fission gas behaviour modelling designed for nuclear fuel performance codes, J. Nucl. Mater. 532 (2020) 152042, https://doi.org/10.1016/j.jnucmat.2020.152042.

[17] P. Van Uffelen, A. Schubert, L. Luzzi, T. Barani, A. Magni, D. Pizzocri, M. Lainet, V. Marelle, B. Michel, S. Boer, S. Lemehov, A. Del Nevo, Incorporation and Verification of Models and Properties in Fuel Performance Codes (754329), INSPYRE, 2020. Deliverable D7.2.

[18] R.L. Williamson, K.A. Gamble, D.M. Perez, S.R. Novascone, G. Pastore, R.J. Gardner, J.D. Hales, W. Liu, A. Mai, Validating the BISON fuel performance code to integral LWR experiments, Nucl. Eng. Des. 301 (2016) 232–244, https://doi.org/10.1016/j.nucengdes.2016.02.020.

[19] D.M. Perez, R.L. Williamson, S.R. Novascone, R.J. Gardner, K.A. Gamble, A.T. Rice, G. Pastore, J.D. Hales, B.W. Spencer, Assessment of BISON: a nuclear fuel performance analysis code, 2015, p. 238. Rev.2 (November).

[20] R.S. Barnes, A theory of swelling and gas release for reactor materials, J. Nucl. Mater. 2 (1964) 135–148.

[21] A.D. Whapham, Electron microscope observation of the fission-gas bubble distribution in UO$_2$, Nucl. Appl. (1966) 123–130, https://doi.org/10.13182/NT66-A27492.

[22] R.J. White, M.O. Tucker, A new fission-gas release model, J. Nucl. Mater. 118 (1) (1983) 1–38, https://doi.org/10.1016/0022-3115(83)90176-9.

[23] C.A. Friskney, M.V. Speight, A calculation on the in-pile diffusional release of fission products forming a general decay chain, J. Nucl. Mater. 62 (1976) 89–94.

[24] R.J. White, The development of grain-face porosity in irradiated oxide fuel, J. Nucl. Mater. 325 (1) (2004) 61–77, https://doi.org/10.1016/

j.jnucmat.2003.10.008.

[25] L.C. Bernard, J.L. Jacoud, P. Vesco, An efficient model for the analysis of fission gas release, J. Nucl. Mater. 302 (2−3) (2002) 125−134, https://doi.org/10.1016/S0022-3115(02)00793-6.

[26] M.S. Veshchunov, Modelling of grain face bubbles coalescence in irradiated UO₂ fuel, J. Nucl. Mater. 374 (1−2) (2008) 44−53, https://doi.org/10.1016/j.jnucmat.2007.06.021.

[27] M.S. Veshchunov, V.D. Ozrin, V.E. Shestak, V.I. Tarasov, R. Dubourg, G. Nicaise, Development of the mechanistic code MFPR for modelling fission-product release from irradiated UO₂ fuel, Nucl. Eng. Des. 236 (2) (2006) 179−200, https://doi.org/10.1016/j.nucengdes.2005.08.006.

[28] A. Booth, A Method of Calculating Fission Gas Diffusion from UO₂ Fuel and its Application to the X-2-F Loop Test, Atomic Energy of Canada Limited, 1957.

[29] S.D. Beck, The Diffusion of Radioactive Fission Products from Porous Fuel Elements, Physics and Mathematics, fifteenth ed., 1960. TID-4500.

[30] J.A. Turnbull, C.A. Friskney, The relation between microstructure and the release of unstable fission products during high temperature irradiation of uranium dioxide, J. Nucl. Mater. 71 (1978) 238−248.

[31] J.A. Turnbull, C.A. Friskney, J.R. Findlay, F.A. Johnson, A.J. Walter, The diffusion coefficients of gaseous and volatile species during the irradiation of uranium dioxide, J. Nucl. Mater. 107 (2−3) (1982) 168−184, https://doi.org/10.1016/0022-3115(82)90419-6.

[32] J.A. Turnbull, R.J. White, C. Wise, The diffusion coefficient for fission gas atoms in uranium dioxide, in: Water Reactor Fuel Element Computer Modelling in Steady State, Transient and Accident Conditions, 1988, pp. 174−181.

[33] P. Van Uffelen, Contribution to the Modelling of Fission Gas Release in Light Water Reactor Fuel, Université de Liège, 2002. Ph.D. thesis.

[34] J.A. Turnbull, The Treatment of Radioactive Fission Gas Release Measurements and Provision of Data for Development and Validation of the ANS-5.4 Model, OECD HALDEN REACTOR PROJECT, 1995.

[35] P.E. Brown, R.L. Faircloth, Metal fission product behaviour in high temperature reactors -UO₂ coated particle fuel, J. Nucl. Mater. 59 (1) (1976) 29−41, https://doi.org/10.1016/0022-3115(76)90005-2.

[36] C. Vitanza, E. Kolstad, U. Graziani, Fission Gas Release from UO₂ Pellet Fuel at High Burn-Up, OECD HALDEN REACTOR PROJECT, 1979, pp. 361−366.

[37] M. Amaya, V. Grismanovs, T. Tverberg, Changes of the surface-to-volume ratio and diffusion coefficient of fission gas in fuel pellets during irradiation, J. Nucl. Mater. 402 (2−3) (2010) 108−115, https://doi.org/10.1016/j.jnucmat.2010.05.004.

[38] A. Claisse, P. Van Uffelen, Towards the inclusion of open fabrication porosity in a fission gas release model, J. Nucl. Mater. 466 (2015) 351−356, https://doi.org/10.1016/j.jnucmat.2015.08.022.

[39] G. Pastore, D. Pizzocri, C. Rabiti, T. Barani, P. Van Uffelen, L. Luzzi, An effective numerical algorithm for intra-granular fission gas release during non-equilibrium trapping and resolution, J. Nucl. Mater. 509 (2018) 687−699, https://doi.org/10.1016/j.jnucmat.2018.07.030.

[40] D. Pizzocri, C. Rabiti, L. Luzzi, T. Barani, P. Van Uffelen, G. Pastore, PolyPole-1: an accurate numerical algorithm for intra-granular fission gas release, J. Nucl. Mater. 478 (2016) 333−342, https://doi.org/10.1016/j.jnucmat.2016.06.028.

[41] National Nuclear Data Center, URL, https://www.nndc.bnl.gov/nudat2/.

[42] M.V. Speight, A calculation on the migration of fission gas in material exhibiting precipitation and Re-solution of gas atoms under irradiation, Nucl. Sci. Eng. 37 (2) (1969) 180−185, https://doi.org/10.13182/nse69-a20676.

[43] F.S. Ham, Theory of diffusion-limited precipitation, J. Phys. Chem. Solid. 6 (4) (1958) 335−351, https://doi.org/10.1016/0022-3697(58)90053-2.

[44] J.A. Turnbull, The distribution of intragranular fission gas bubbles in UO₂ during irradiation, J. Nucl. Mater. 38 (2) (1971) 203−212, https://doi.org/10.1016/0022-3115(71)90044-4.

[45] D.R. Olander, D. Wongsawaeng, Re-solution of fission gas - a review: Part I. Intragranular bubbles, J. Nucl. Mater. 354 (1−3) (2006) 94−109, https://doi.org/10.1016/j.jnucmat.2006.03.010.

[46] W.L. Oberkampf, T.G. Trucano, C. Hirsch, Verification, validation, and predictive capability in computational engineering and physics, Appl. Mech. Rev. 57

[47] (1−6) (2002) 345−384, https://doi.org/10.1115/1.1767847.

[47] M.S. Veshchunov, On the theory of fission gas bubble evolution in irradiated UO₂ fuel, J. Nucl. Mater. 277 (2000) 67−81.

[48] M.V. Speight, W.B. Beeré, Vacancy potential and void growth on grain boundaries, Met. Soc. 9 (1975) 190−191.

[49] G.L. Reynolds, W.B. Beeré, P.-T. Sawbridge, The effect of fission products on the ratio of grain-boundary energy to surface energy in irradiated uranium dioxide, J. Nucl. Mater. 41 (1971) 112−114.

[50] D.R. Olander, Fundamental Aspects of Nuclear Reactor Fuel Elements, Technical Information Center Energy Research and Development Administration, 1976.

[51] D.A. Andersson, M.R. Tonks, L. Casillas, S. Vyas, P. Nerikar, B.P. Uberuaga, C.R. Stanek, Multiscale simulation of xenon diffusion and grain boundary segregation in UO₂, J. Nucl. Mater. 462 (2015) 15−25, https://doi.org/10.1016/J.JNUCMAT.2015.03.019.

[52] D.A. Andersson, P. Garcia, X.Y. Liu, G. Pastore, M. Tonks, P. Millett, B. Dorado, D.R. Gaston, D. Andrs, R.L. Williamson, R.C. Martineau, B.P. Uberuaga, C.R. Stanek, Atomistic modeling of intrinsic and radiation-enhanced fission gas (Xe) diffusion in UO2±x: implications for nuclear fuel performance modeling, J. Nucl. Mater. 451 (1−3) (2014) 225−242, https://doi.org/10.1016/J.JNUCMAT.2014.03.041.

[53] A. Jelea, R.J. Pellenq, F. Ribeiro, An atomistic modeling of the xenon bubble behavior in the UO₂ matrix, J. Nucl. Mater. 444 (1−3) (2014) 153−160, https://doi.org/10.1016/J.JNUCMAT.2013.09.041.

[54] C.R. Stanek, R.W. Grimes, M.R. Bradford, Segregation of fission products to surfaces of UO2, Mater. Res. Soc. Symp. Proc. 654 (1) (2001). AA3.32.1−AA3.32.6. doi:10.1557/proc-654-aa3.32.1. URL, https://link.springer.com/article/10.1557/PROC-654-AA3.32.1.

[55] R.M. Carroll, J.G. Morgan, R.B. Perez, O. Sisman, Fission density, burnup, and temperature effects on fission-gas release from UO₂, Nucl. Sci. Eng. 38 (1969) 143−155, https://doi.org/10.13182/NSE69-A19519. URL, https://www.tandfonline.com/doi/abs/10.13182/NSE69-A19519.

[56] J. Rest, S.M. Gehl, The mechanistic prediction of transient fission-gas release from LWR fuel, Nucl. Eng. Des. 56 (1) (1980) 233−256, https://doi.org/10.1016/0029-5493(80)90189-2.

[57] C.T. Walker, P. Knappik, M. Mogensen, Concerning the development of grain face bubbles and fission gas release in UO₂ fuel, J. Nucl. Mater. 160 (1) (1988) 10−23, https://doi.org/10.1016/0022-3115(88)90003-7.

[58] T. Barani, E. Bruschi, D. Pizzocri, G. Pastore, P. Van Uffelen, R.L. Williamson, L. Luzzi, Analysis of transient fission gas behaviour in oxide fuel using BISON and TRANSURANUS, J. Nucl. Mater. 486 (2017) 96−110, https://doi.org/10.1016/j.jnucmat.2016.10.051.

[59] T. Kogai, Modelling of fission gas release and gaseous swelling of light water reactor fuels, J. Nucl. Mater. 244 (2) (1997) 131−140, https://doi.org/10.1016/S0022-3115(96)00731-3.

[60] M. Charles, J.J. Abassin, D. Baron, M. Bruet, P. Melin, Utilization of contact experiments to improve the fission gas release knowledge in Pwr fuel rods, in: IAEA Specialists Meetiing on Fuel Element Performance Computer Modelling, 1983, pp. 1−18. Preston.

[61] M. Bruet, J. Dodelier, P. Melin, M.-L. Pointund, CONTACT 1 and 2 experiments: behaviour of PWR fuel rod up to 15000 MWd/tU, in: IAEA Specialists' Meeting on Water Reactor Fuel Element Performance Computer Modelling, 1980, pp. 235−244.

[62] I.J. Hastings, C.E.L. Hunt, J.J. Lipsett, R.D. Delaney, Short-lived fission product release from the surface and centre of operating UO₂ fuel, in: Water Reactor Fuel Element Performance Computer Modelling, IAEA, 1984, pp. 416−425.

[63] I.J. Hastings, C.E.L. Hunt, J.J. Lipsett, R.D. MacDonald, Behaviour of short-lived fission products within operating UO₂ fuel elements, Res. Mech. 6 (3) (1983).

[64] T. Barani, D. Pizzocri, F. Cappia, L. Luzzi, G. Pastore, P. Van Uffelen, Modeling high burnup structure in oxide fuels for application to fuel performance codes. part I: high burnup structure formation, J. Nucl. Mater. 539 (2020), https://doi.org/10.1016/j.jnucmat.2020.152296.